PHOTON-INDUCED PROCESSES IN SEMI-CENTRAL NUCLEUS–NUCLEUS COLLISIONS*

Antoni Szczurek

Institute of Nuclear Physics Polish Academy of Sciences
31-342 Kraków, Poland
and
University of Rzeszów, Pigonia 1, 35-310 Rzeszów, Poland

(Received March 26, 2019)

We calculate total and differential cross sections for J/ψ photoproduction in ultrarelativistic lead–lead collisions at the LHC energy $\sqrt{s_{NN}} = 2.76$ TeV. We use a simple model based on vector dominance picture and multiple scattering of the hadronic $(c\bar{c})$ state in a cold nucleus. In our analysis, we use Glauber formulae for calculating $\sigma_{\mathrm{tot},J/\psi\mathrm{Pb}}$ which is a building block of our model. For semi-central collisions, a modification of the photon flux is necessary. We discuss how to effectively correct photon fluxes for geometry effects. We try to estimate the cross sections for different centrality bins and for J/ψ mesons emitted in forward rapidity range $(2.5 < y < 4)$ corresponding to the ALICE experimental results. We discuss similar analysis for dilepton production in ultrarelativistic heavy-ion collisions at very low pair transverse momenta, $P_{\mathrm{T}} \leq 0.15\,\mathrm{GeV}$. We investigate the interplay of thermal radiation with photon annihilation processes, $\gamma\gamma \to l^+l^-$, due to the coherent electromagnetic fields of the colliding nuclei. For the thermal radiation, we employ the emission from the QGP and hadronic phases with in-medium vector spectral functions. We first verify that the combination of photon fusion, thermal radiation and final-state hadron decays gives a fair description of the low-P_{T} invariant-mass as well as P_{T} distributions as measured recently by the STAR Collaboration in $\sqrt{s_{NN}} = 200\,\mathrm{GeV}$ Au+Au collisions for different centralities. The coherent contribution dominates in peripheral collisions, while thermal radiation shows a significantly stronger increase with centrality. We also provide predictions for the ALICE experiment at the LHC. The resulting excitation function reveals a nontrivial interplay of photoproduction and thermal radiation.

DOI:10.5506/APhysPolB.50.1263

* Presented at the Cracow Epiphany Conference on Advances in Heavy Ion Physics, Kraków, Poland, January 8–11 2019.

1. Introduction

The J/ψ production in heavy-ion collisions was considered as a flag example of quark–gluon plasma. Simultaneously, J/ψ was studied in ultraperipheral collisions when nuclei do not touch. In this case, a coherent photon, which couples to one of the colliding nuclei, fluctuates into a virtual J/ψ or $c\bar{c}$ pair which then is produced as J/ψ meson in the final state. Till recently, it was not discussed what happens to the photoproduction processes when nuclei collide and presumably quark–gluon plasma is created. Quite recently, the ALICE Collaboration observed J/ψ with very small transverse momenta in peripheral and semi-central collisions [1]. This was interpreted in [2] as an effect of photoproduction mechanism which is active also in such a case.

Lately, the STAR Collaboration observed also enhanced production of dielectron pairs with small transverse momenta [3]. We showed very recently [4] that this may be interpreted as $\gamma\gamma \to e^+e^-$ processes (with coherent photons) even in the semi-central collisions.

In this presentation, we discuss what happens with the coherent photon-induced processes in the semi-central collisions. Two examples are presented:

(a) photoproduction of J/ψ meson,

(b) production of dilepton pairs.

2. Sketch of the formalism

2.1. J/ψ production

We start from the presentation of the situation for J/ψ meson production in semi-central collisions. In Fig. 1, we show the situation in the impact parameters space. Either the first or the second ion emits a photon. The corresponding hadronic fluctuation rescatters then in the second or first nucleus, respectively.

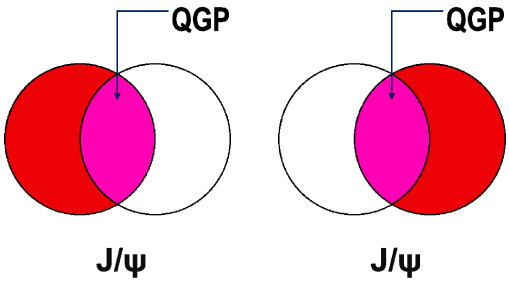

Fig. 1. (Color online) Emission of J/ψ — a picture in the plane x, y perpendicular to the collision axis (z). In the light gray (pink) area quark–gluon plasma is created.

In Fig. 2, we compare a situation for ultraperipheral (left) and semi-central (right) collisions. Is J/ψ created before nuclear collision? If yes, it would be easy to destroy J/ψ in the quark–gluon plasma (light gray/orange).

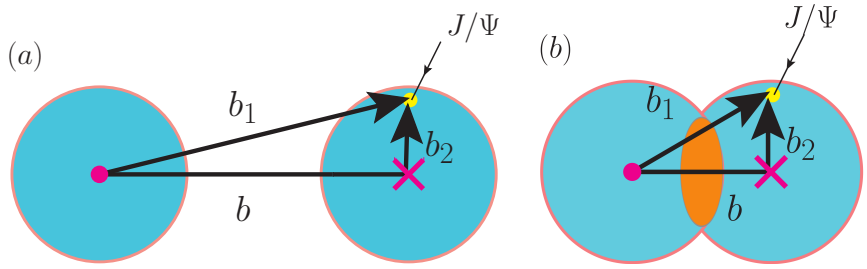

Fig. 2. (Color online) Impact parameter picture of the production of the J/ψ meson for ultraperipheral (left panel) and for semi-central (right panel) collisions. It is assumed here that the first nucleus is the emitter of the photon which rescatters then in the second nucleus being a rescattering medium.

The details how to calculate the cross section were exposed in [2]. We proposed that compared to UPC collisions, one should modify photon flux factors. The effective photon flux, which includes the geometrical aspects, can be formally expressed through the real photon flux of one of the nuclei and effective strength for the interaction of the photon with the second nucleus

$$N^{(1)}\left(\omega_1, b\right) = \int N\left(\omega_1, b_1\right) \frac{\theta\left(R_A - \left(\left|\vec{b}_1 - \vec{b}\right|\right)\right)}{\pi R_A^2} \, \mathrm{d}^2 b_1 \,, \tag{1}$$

where $\vec{b}_1 = \vec{b} + \vec{b}_2$. The extra $\theta(R_A - (|\vec{b}_1 - \vec{b}|))$ factor ensures collision, when the photon hits the nucleus-medium. For the photon flux in the second nucleus one needs to replace $1 \to 2$ (and $2 \to 1$). For large $b \gg R_A + R_B$: $N^{(1)}\left(\omega_1, b\right) \approx N(\omega_1, b)$. For small impact parameters, this approximation is, however, not sufficient. This has some consequences also for ultraperipheral collisions, which will be discussed somewhat later in this section. Since it is not completely clear what happens in the region of overlapping nuclear densities, we suggest another approximation, which may be considered rather as lower limit. In this approximation, we integrate the photon flux of the first (emitter) nucleus only over this part of the second (medium) nucleus, which does not collide with the nucleus-emitter (some extra absorption may be expected in the tube of overlapping nuclei). This may decrease the cross section for more central collisions. In particular, for the impact parameter $b = 0$, the resulting vector meson production cross section will fully disappear by the construction. In the above approximation, the photon flux can

be written as

$$N^{(2)}\left(\omega_1, b\right) = \int N\left(\omega_1, b_1\right) \frac{\theta\left(R_A - \left(\left|\vec{b}_1 - \vec{b}\right|\right)\right) \times \theta(b_1 - R_A)}{\pi R_A^2} \mathrm{d}^2 b_1 \,. \quad (2)$$

In our calculation, we use the following generic formula for calculating the photon flux for any nuclear form factor (denoted F below):

$$N(\omega, b) = \frac{Z^2 \alpha_{\mathrm{em}}}{\pi^2} \left| \int u^2 J_1\left(u\right) \frac{F\left(\frac{\left(\frac{\omega b}{\gamma}\right)^2 + u^2}{b^2}\right)}{\left(\frac{\omega b}{\gamma}\right)^2 + u^2} \right|^2 . \quad (3)$$

The fluxes including different limitations are shown in Fig. 3.

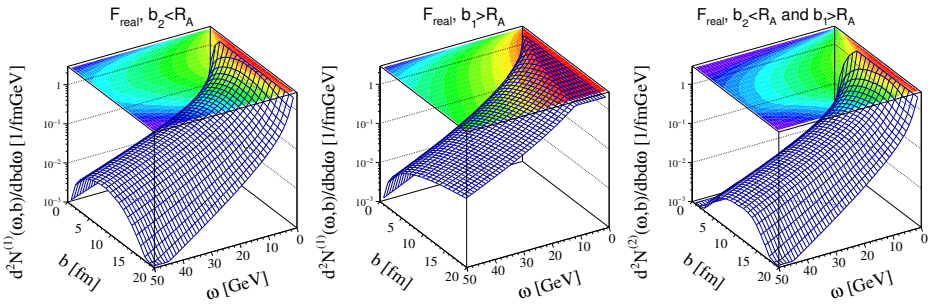

Fig. 3. Two-dimensional distributions of the photon flux in the impact parameter b and in the energy of photon ω for three different conditions (more in the text).

2.2. Dilepton production

The general picture in the impact parameter space is shown in Fig. 4. There are general questions one can add concerning the considered reaction. Is e^+e^- created before nuclear collision? Can plasma/spectators distort distributions of leptons? Here, a big fraction of events can be produced outside (in the impact parameter space) of both colliding nuclei (the dark area). Therefore, not big difference of the cross sections between UPC and non-UPC is expected.

The main ingredient for the photon–photon fusion mechanism is the flux of photons for an ion of charge Z moving along impact parameter with the relativistic parameter γ. With the nuclear charge form factor F_{em} as an

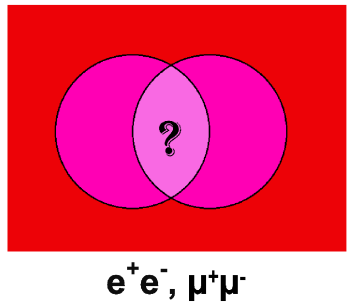

Fig. 4. Dilepton production — a picture in the x, y plane perpendicular to the collision axis (z). The area with the question mark is the region where quark–gluon plasma is created.

input, the flux can be calculated as in [5, 6]

$$N(\omega, b) = \frac{Z^2 \alpha_{\mathrm{em}}}{\pi^2} \left| \int_0^\infty \mathrm{d}q_{\mathrm{T}} \frac{q_{\mathrm{T}}^2 F_{\mathrm{em}} \left(q_{\mathrm{T}}^2 + \frac{\omega^2}{\gamma^2} \right)}{q_{\mathrm{T}}^2 + \frac{\omega^2}{\gamma^2}} J_1(b q_{\mathrm{T}}) \right|^2 , \tag{4}$$

where J_1 is a Bessel function, q_{T} is photon transverse momentum and ω is photon energy. We calculate the form factor from the Fourier transform of the nuclear charge density.

The differential cross section for dilepton (l^+l^-) production via $\gamma\gamma$ fusion at fixed impact parameter of a nucleus–nucleus collision can then be written as

$$\frac{\mathrm{d}^2\sigma_{ll}}{\mathrm{d}\xi \mathrm{d}^2 b} = \int \mathrm{d}^2 b_1 \mathrm{d}^2 b_2 \, \delta^{(2)} \left(\vec{b} - \vec{b}_1 - \vec{b}_2 \right) N(\omega_1, b_1) N(\omega_2, b_2) \frac{\mathrm{d}\sigma(\gamma\gamma \to l^+l^-; \hat{s})}{\mathrm{d}p_{\mathrm{T}}^2} , \tag{5}$$

where the phase space element is $\mathrm{d}\xi = \mathrm{d}y_+ \mathrm{d}y_- \mathrm{d}p_{\mathrm{T}}^2$ with $y_\pm$, p_{T} and m_l the single-lepton rapidities, transverse momentum and mass, respectively, and

$$\begin{aligned} \omega_1 &= \frac{\sqrt{p_{\mathrm{T}}^2 + m_l^2}}{2} \left(e^{y_+} + e^{y_-} \right) , \\ \omega_2 &= \frac{\sqrt{p_{\mathrm{T}}^2 + m_l^2}}{2} \left(e^{-y_+} + e^{-y_-} \right) , \\ \hat{s} &= 4\omega_1\omega_2 . \end{aligned} \tag{6}$$

As can be seen from Eq. (4), the transverse momenta, q_{T}, of the photons have been integrated out, and in this approximation, dileptons are produced back-to-back in the transverse plane.

In UPCs, the incoming nuclei do not touch, *i.e.* no strong interactions occur between them. In this case, one usually imposes the constraint $b > 2R_A$, when integrating over impact parameter. In semi-central collisions, we lift this restriction allowing the nuclei to collide.

An exact calculation of the pair-$p_{\rm T}$ dependence is, in general, rather involved. In Ref. [4], we performed a simplified calculation using b-integrated transverse-momentum-dependent photon fluxes

$$\frac{{\rm d}^2N\left(\omega, q_{\rm T}^2\right)}{{\rm d}^2\vec{q}_{\rm T}} = \frac{Z^2\alpha_{\rm em}}{\pi^2}\frac{q_{\rm T}^2}{\left[q_{\rm T}^2 + \frac{\omega^2}{\gamma^2}\right]^2}F_{\rm em}^2\left(q_{\rm T}^2 + \frac{\omega^2}{\gamma^2}\right) . \tag{7}$$

The $p_{\rm T}$ distribution is then obtained as the convolution of two transverse-momentum-dependent photon fluxes with the elementary $\gamma\gamma \to e^+e^-$ cross section

$$\frac{{\rm d}^2\sigma_{ll}}{{\rm d}^2\vec{P}_{\rm T}} = \int \frac{{\rm d}\omega_1}{\omega_1}\frac{{\rm d}\omega_2}{\omega_2}{\rm d}^2\vec{q}_{1\rm T}\,{\rm d}^2\vec{q}_{2\rm T}$$
$$\times\frac{{\rm d}^2N\left(\omega_1, q_{1\rm T}^2\right)}{{\rm d}^2\vec{q}_{1\rm T}}\frac{{\rm d}^2N\left(\omega_2, q_{2\rm T}^2\right)}{{\rm d}^2\vec{q}_{2\rm T}}\delta^{(2)}\left(\vec{q}_{1\rm T} + \vec{q}_{2\rm T} - \vec{P}_{\rm T}\right)\hat{\sigma}(\gamma\gamma \to l^+l^-)\Big|_{\rm cuts} , \tag{8}$$

The resulting shape of integrated cross section is then renormalized to the previously obtained cross section within the collinear approximation for a given centrality class.

3. Selected results

In Fig. 5, we show the nuclear cross section for J/ψ production as a function of the impact parameter also for $b < R_A + R_B$, *i.e.* for the semi-central collisions. We show results for a broad range of impact parameter ($0 < b < R_A + R_B$). However, the application of our approach for very small b is not obvious.

The different lines correspond to different approximations of photon fluxes within our approach as described in the figure caption. The dashed and solid lines represent upper and lower limit for the cross section. At larger values of impact parameter b, the cross sections obtained with the different fluxes practically coincide. At $b < R_A + R_B$, the different approximations give quite different results. The standard approach in the literature for UPC when naively applied to the semi-central collisions overestimates the cross section.

We summarize our calculations in [2] in Fig. 6. We present both statistical and systematic error bars (shaded area). We show our results starting from centralities bigger than 30%. As discussed above, we do not trust our

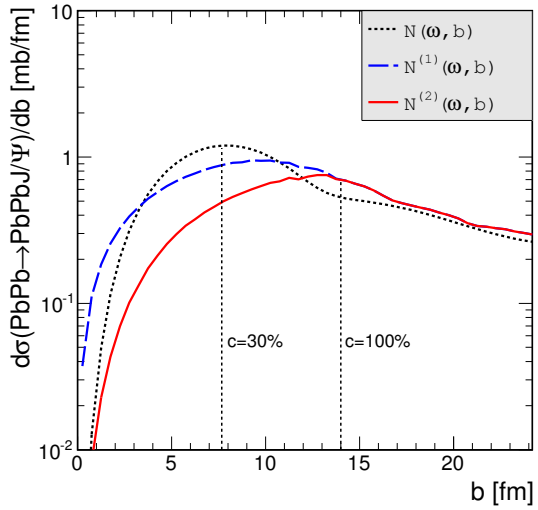

Fig. 5. Differential cross section for photoproduction of J/ψ meson as a function of impact parameter for $\sqrt{s_{NN}} = 2.76$ TeV. Different lines correspond to different approximations: dotted — standard UPC approach, dashed — first approximation/correction (upper limit), solid — second approximation/correction (lower limit). Here, realistic (charge) nuclear form factor was used. For reference, we show vertical lines corresponding to centralities $c = 30\%$ and $c = 100\%$.

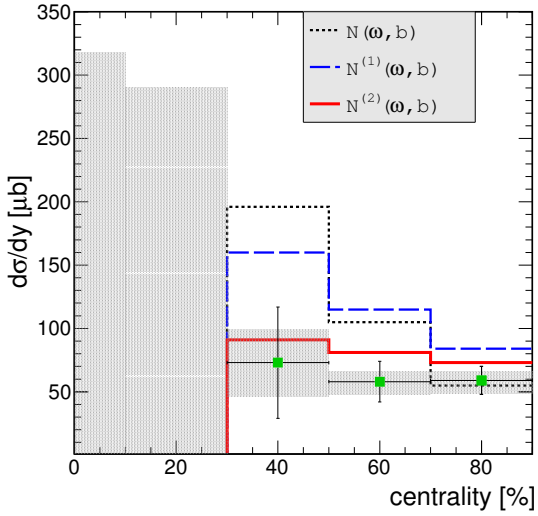

Fig. 6. $\Delta\sigma/\Delta y$ cross sections for different centrality bins. Theoretical results for different models of the photon flux are compared with the ALICE data [1]. The shaded area represents the experimental uncertainties.

results for lower centralities. In addition, the ALICE Collaboration could not extract actual values of the cross section for the two lowest centrality bins. The results for standard photon flux exceed the ALICE data. Rather good agreement with the data is achieved for the $N^{(2)}$ photon flux obtained with the realistic nucleus form factor.

In Fig. 7, we show dielectron invariant-mass spectra for small pair $p_{\rm T} < 0.15$ GeV and three different centrality classes as selected in the STAR analysis: peripheral (60–80%), semi-peripheral (40–60%) and semi-central (10–40%) collisions. We also include the experimental acceptance cuts on the single-lepton tracks as applied by STAR, and take the cocktail contribution as provided by STAR [3] representing the final-state decays of the produced hadrons. In peripheral collisions, the photon–photon contribution dominates while in semi-central collisions, all three contributions are of similar magnitude. Their sum yields a rather good agreement with the STAR data, except for the J/ψ peak region. Our calculations only contain incoherent J/ψ production, from binary nucleon–nucleon collisions; we conjecture that the missing contribution is due to a coherent contribution [2].

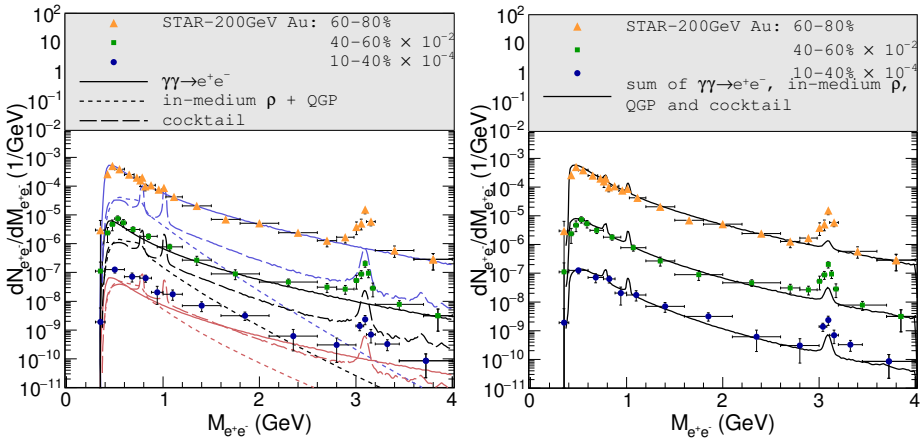

Fig. 7. Left: Dielectron invariant-mass spectra for pair-$p_{\rm T} < 0.15$ GeV in Au+Au ($\sqrt{s_{NN}} = 200$ GeV) collisions for 3 centrality classes including experimental acceptance cuts ($p_{\rm T} > 0.2$ GeV, $|\eta_e| < 1$ and $|y_{e^+e^-}| < 1$) for $\gamma\gamma$ fusion (solid lines), thermal radiation (dotted lines) and the hadronic cocktail (dashed lines). Right: Comparison of the total sum (solid lines) to the STAR data [3].

We also calculated the pair-$P_{\rm T}$ distributions for the $\gamma\gamma$ fusion mechanism and combine it with the ones from thermal radiation and the cocktail in Fig. 8. One can clearly identify the low-$P_{\rm T}$ region where the $\gamma\gamma$ fusion dominates, although the width of the low-$P_{\rm T}$ peak in the data is slightly smaller

than for the data. In our calculations, we used the realistic nuclear form factor from Ref. [7], which leads to the oscillations in the p_{T} distributions for the coherent photon mechanism.

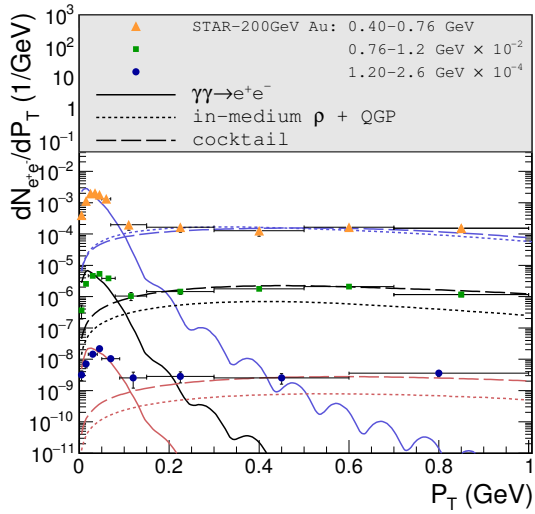

Fig. 8. p_{T} spectra of the individual contributions (line styles as in the previous figure) in 3 different mass bins for the 60–80% centrality of the Au+Au collisions ($\sqrt{s_{NN}} = 200\,\mathrm{GeV}$), compared to the STAR data [3].

In Fig. 9, we show our predictions for the two sources for Pb+Pb collisions at $\sqrt{s_{NN}} = 5.02\,\mathrm{TeV}$ for the same centrality classes and single-lepton acceptance cuts as for our RHIC calculations. Compared to the latter, the picture is qualitatively similar, although the strength of thermal contribution is relatively stronger, especially in semi-peripheral and central collisions, where it is comparable and even larger than the $\gamma\gamma$ yield at low mass.

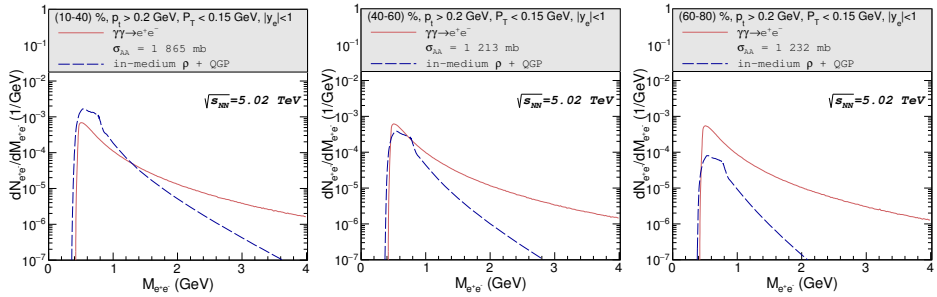

Fig. 9. Our predictions for low-p_{T} dilepton radiation in Pb+Pb ($\sqrt{s_{NN}} = 5.02\,\mathrm{TeV}$) collisions from coherent $\gamma\gamma$ fusion (solid lines) and thermal radiation (dashed lines) for three centrality classes and acceptance cuts as specified in the figures.

In Fig. 10, we present the dependence of the two different contributions (total cross section) for selected centrality classes as a function of $\sqrt{s}$. While at low energies, the photon-fusion mechanism is negligible, it quickly rises with energy and saturates at about RHIC energies. In contrast, the thermal contribution grows gradualy with energy. This plot shows that the RHIC energy $\sqrt{s_{NN}} = 200$ GeV is the most favorable for observing the photon–photon fusion.

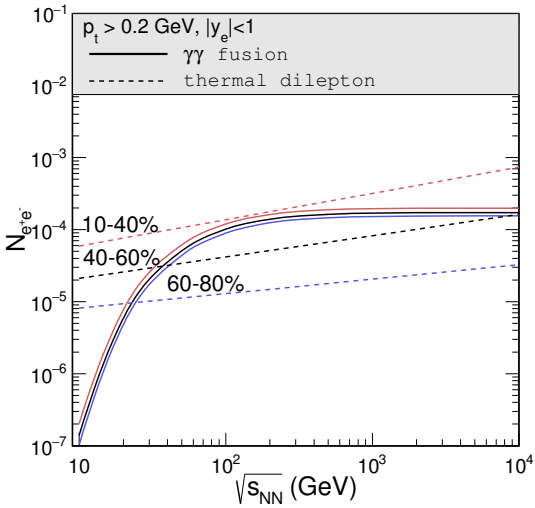

Fig. 10. Excitation function of low-P_{T} (< 0.15 GeV) dilepton yields from $\gamma\gamma$ fusion (solid lines) and thermal radiation (dashed lines) in collisions of heavy nuclei ($A \simeq 200$) around midrapidity in three centrality classes, including single-$e^{\pm}$ acceptance cuts.

4. Conclusions

We have presented a theoretical study of photoproduction mechanism in the case when nuclei collide and produce quark–gluon plasma and as a consequence considerable number of hadrons is produced. On theoretical side, the nuclear photoproduction in UPC was treated in the equivalent photon approximation with photon fluxes and photon–nucleus cross section being the basic ingredients of the approach.

We have assumed that the whole nucleus produces photons. The photon (or hadronic photon fluctuation) must hit the other nucleus to produce the J/ψ meson.

The question arises how to treat the region of overlapping colliding nuclei in the impact parameter space where some absorption of J/ψ may be expected. We include the effect of the "absorption" by modifying effective

photon fluxes in the impact parameter space by imposing additional geometrical conditions on impact parameters (between photon and nuclei and/or between colliding nuclei).

As an example, we have considered a vector-dominance-based model which includes multiple scattering effects. Any other model/approach can be applied in the future.

By modifying standard photon fluxes valid for UPC by collision geometry, we have calculated the cross section for different centrality bins relevant for the ALICE Collaboration analysis. Our results have been compared with their data. We have obtained a reasonable agreement for peripheral and semi-central collisions and set limits for the cross section for the semi-central collisions.

Our lower limit is, however, somewhat model-dependent. Since in our calculations we have used coherent $\gamma A \to J/\psi A$ cross section, our lower limit may be overestimated especially for small impact parameters.

The time picture of the whole process is not clear to us at the moment. The rather reasonable agreement of our quite simplified approach with the ALICE data suggests that the "coherent" (assumed by the formula used for the $\gamma A \to J/\psi A$ process) scattering of the hadronic fluctuation happens before the nucleus undergoes the process of deterioration due to nucleus–nucleus collision and before the quark–gluon plasma is created.

Here, we have discussed the analysis for a forward rapidity range. There the J/ψ quarkonia are emitted forward with large velocity, therefore, they could potentially escape from being melted in the quark–gluon plasma. At midrapidities, the situation could be slightly different. The ALICE Collaboration would repeat their analysis also in the midrapidity range and verify the $P_{\mathrm{T}} \approx 0$ enhancement.

We have discussed also low-P_{T} dilepton production in ultrarelativistic heavy-ion collisions, by conducting systematic comparisons of the two sources of dileptons. The former was taken from a model including in-medium hadronic and QGP emission rates, while the latter was calculated utilizing photon fluxes with realistic nuclear form factors including the case of nuclear overlap. We have found that the combination of the two sources (augmented by a contribution from the hadronic final-state decay cocktail) gives a good description of low-p_{T} dilepton data in Au–Au ($\sqrt{s_{NN}} = 200\,\mathrm{GeV}$) collisions in three centrality classes for invariant masses from the threshold to 4 GeV (with the exception of the J/ψ peak related to coherent production of J/ψ). The coherent emission of e^+e^- pairs was found to be dominant for the two peripheral samples, and comparable to the cocktail and thermal radiation yields in semi-central collisions.

At high energies, the situation is similar to RHIC energies. The interplay of these processes at the LHC is of particular interest in view of plans by the ALICE Collaboration [8] to lower the single-electron p_{T} cuts and measure very-low mass spectra.

We have summarized our results in an excitation function of low-p_{T} radiation covering three orders of magnitude in collision energy. While coherent production increases rather sharply, and then levels off near $\sqrt{s_{NN}} \simeq 100\,\mathrm{GeV}$, thermal radiation increases more gradually with $\sqrt{s_{NN}}$. This explains why the latter is dominant at the SPS, the former dominates at RHIC, and the latter becomes more important again at the LHC.

I am indebted to Mariola Kłusek-Gawenda, Ralf Rapp and Wolfgang Schäfer for collaboration on the issues presented here.

REFERENCES

[1] E.L. Kryshen [ALICE Collaboration], *Nucl. Phys. A* **967**, 273 (2017).
[2] M. Kłusek-Gawenda, A. Szczurek, *Phys. Rev. C* **93**, 044912 (2016).
[3] J. Adam *et al.* [STAR Collaboration], *Phys. Rev. Lett.* **121**, 132301 (2018).
[4] M. Kłusek-Gawenda, R. Rapp, W. Schäfer, A. Szczurek, *Phys. Lett. B* **790**, 339 (2019).
[5] C.A. Bertulani, G. Baur, *Phys. Rep.* **163**, 299 (1988).
[6] G. Baur *et al.*, *Phys. Rep.* **364**, 359 (2002).
[7] S.R. Klein *et al.*, *Comput. Phys. Commun.* **212**, 258 (2017).
[8] F. Antinori, P. Braun-Munzinger, S. Flörchinger, private communication, 2018.